

## Photon-stimulated desorption of fluorine from silicon via substrate core excitations

Jory A. Yarmoff and Stephen A. Joyce

*Surface Science Division, National Institute of Standards and Technology,\* Gaithersburg, Maryland 20899*

(Received 20 March 1989)

Photon-stimulated desorption (PSD) of  $F^+$  was performed for silicon (111) surfaces terminated with fluorine atoms. The surfaces were prepared by exposure of clean silicon to  $XeF_2$ . The onset for PSD at the Si  $2p$  edge correlated with the transition from the  $2p$  level of the bonding silicon atom to the conduction-band minimum, and was thus a function of the oxidation state of the bonding atom. The ions originating from a SiF surface species desorbed along the surface normal while the ions from a SiF<sub>3</sub> group desorbed in off-normal directions. Localized  $3s$  and  $3p$  Rydberg-like resonances were observed in the quasimolecular SiF<sub>3</sub> moieties. The ion kinetic-energy distributions were measured as an aid to elucidating the desorption mechanism. Measurements of the PSD of  $F^+$  at the Si  $2s$  edge were used to confirm the  $3s$  and  $3p$  character of the measured resonances.

### I. INTRODUCTION

Photon-stimulated desorption (PSD) has been long recognized to be a viable technique for the determination of the local electronic structure of adsorbates on surfaces.<sup>1-3</sup> This is due to the inherent surface sensitivity of PSD in combination with the detection selectivity. In a previous paper<sup>4</sup> we showed how PSD of  $F^+$  from a silicon surface is a chemically selective process, i.e., the thresholds for PSD observed at the substrate core-level edge coincide with the oxidation state of the bonding surface atom. This paper presents a much more detailed analysis of the chemically selective nature of PSD in this system.

Since it is possible to prepare silicon surfaces with a variety of surface fluoride species,<sup>5</sup> the fluorine-on-silicon system is ideal for displaying the various factors important in chemically selective stimulated desorption. Because the bonding is fairly ionic, desorption can be easily induced via core-hole excitation, thus allowing the PSD spectra to be used as a measure of the local electronic structure associated with the bonding atom. Because of the high yield of fluorine ions, measurements of both the excitation-energy dependence and the resulting ion kinetic energies can be easily obtained.

In this paper, PSD spectra taken at the Si  $2p$  and  $2s$  edges are presented. As will be shown, the details of the PSD process are dependent on the structure of both the initial and final electronic states of the transition used to initiate the desorption event. In Sec. II we will briefly outline the experimental details, in Sec. III we will present the results and a discussion, and in Sec. IV we will list our major conclusions.

### II. EXPERIMENT

These experiments were performed on beamline UV-8b at the National Synchrotron Light Source (NSLS) at Brookhaven National Laboratory (Upton, NY). Si(111) wafers, cut within  $0.25^\circ$  of the low-index plane, were cleaned via standard methods<sup>6</sup> in ultrahigh vacuum

(UHV). Cleanliness was checked by monitoring the surface core-level shifts and the valence-band surface states with photoemission.

The surfaces were exposed to fluorine by transferring them under UHV into a separate reaction chamber (base pressure  $1 \times 10^{-9}$  Torr), and then exposing them to 50 L (1 L = 1 langmuir  $\equiv 1 \times 10^{-6}$  Torr sec) of  $XeF_2$ .<sup>5</sup> Following exposure, the samples were transferred back into the spectrometer chamber (base pressure  $1 \times 10^{-11}$  Torr). The composition of the surfaces was measured via Si  $2p$  core-level photoemission, employing an ellipsoidal mirror analyzer<sup>7</sup> (EMA) with a typical energy resolution (combined monochromator and spectrometer) of 0.1 eV.

PSD was measured by reversing the polarity of the optics so as to be sensitive to ions instead of electrons, and then biasing the entrance to the multichannel-plate array by  $-1000$  V to provide additional acceleration of the ions. In this manner it was possible to collect both kinetic-energy distributions of the emitted ions and the dependence of the ion yield on the incident-photon energy. For collecting PSD spectra, the resolution of the incident-photon beam was degraded (to  $\sim 0.4$  eV) from that used for photoemission in order to increase the signal level. This did not degrade the quality of the spectra, however, as none of the features in the PSD yield curves were  $< 0.5$  eV wide. The PSD signal was normalized, to account for the monochromator output and for drifts in the beam current, by dividing the ion signal by the total photocurrent measured at the gold-coated final focusing mirror. Also, since the only ion to desorb from a fluorine-terminated silicon surface is  $F^+$ , as determined by electron-stimulated-desorption (ESD) experiments employing mass analysis,<sup>8-10</sup> we did not use any mass discrimination in the present study.

The EMA collects ions emitted within an  $\sim 85^\circ$  cone. In our previous study,<sup>4</sup> we had measured the angular dependence of the emitted ions by collecting spectra with the sample surface normal to the EMA and by rotating the crystal so as to be more sensitive to the ions exiting the surface at a near grazing angle and less sensitive to the ions emitted in the normal direction. A problem with

Work of the U. S. Government  
Not subject to U. S. copyright

this method was that the intensity of the desorbed ions in the off-normal direction was severely restricted by the analyzer geometry, therefore requiring extremely long data-collection periods. To measure the angular dependence of the emitted ions in the present study, we have instead applied a bias of  $-75$  V to the first grid in the EMA. This bias voltage has no effect on the energy distributions measured with the analyzer, but does have the effect of compressing the total emitted ion signal into the acceptance region of the detector. This technique is commonly employed for collecting electron-stimulated-desorption ion angular distributions.<sup>11</sup> The data collected with the bias on are thus the ion yield emitted over all angles. The portion of the signal associated with off-normal ion emission can then be ascertained by comparison with the residual normal emission (bias off). Note that although the EMA has been used for angle-resolved measurements,<sup>12</sup> this capability was not employed for the present results.

### III. RESULTS AND DISCUSSION

The photoemission spectra of the two surfaces employed for these studies, collected with 130 eV incident-photon energy, are shown in Fig. 1. The squares show the raw data after subtraction of a background that was obtained by a spline fit to the regions on both sides of the photoemission peaks. The solid line is the result of a numerical fit to the data in a manner previously described,<sup>5,13</sup> and the dashed lines show the individual components of the fit. Each of these is represented by a Gaussian-broadened Lorentzian line shape that is composed of the sum of the spin-orbit-split components of the Si 2*p* core level, using 0.61 eV and 0.52 eV as the splitting and the branching ratio, respectively.

The surfaces used in the present study were prepared by exposure of a clean Si(111)-(7×7) surface to 50 L of XeF<sub>2</sub> at room temperature. This produces a surface composed primarily of mono- and trifluoride units, with a small amount of SiF<sub>2</sub>, as shown in Fig. 1(a). Note that the addition of each fluorine bond results in a chemical shift of the Si 2*p* level of approximately 1 eV.<sup>5</sup> Another surface composition was produced by annealing to approximately 300°C, which induces the desorption of some of the fluorine, leaving a surface terminated primarily by SiF moieties.<sup>4</sup> The photoemission spectrum of this surface is shown in Fig. 1(b). In the interests of developing a coherent presentation of these results, we will first discuss the annealed surface, since the surface composed primarily of monofluoride species is considerably simpler to understand spectroscopically than the surface containing multiple fluorides.

The density of unoccupied electronic states associated with this surface composition contributes to the absorption and PSD excitation spectra at the Si 2*p* core level, as shown in Fig. 2. The absorption spectrum, shown as a dashed line, was collected by measuring the yield of secondary electrons with a kinetic energy of 20 eV. This

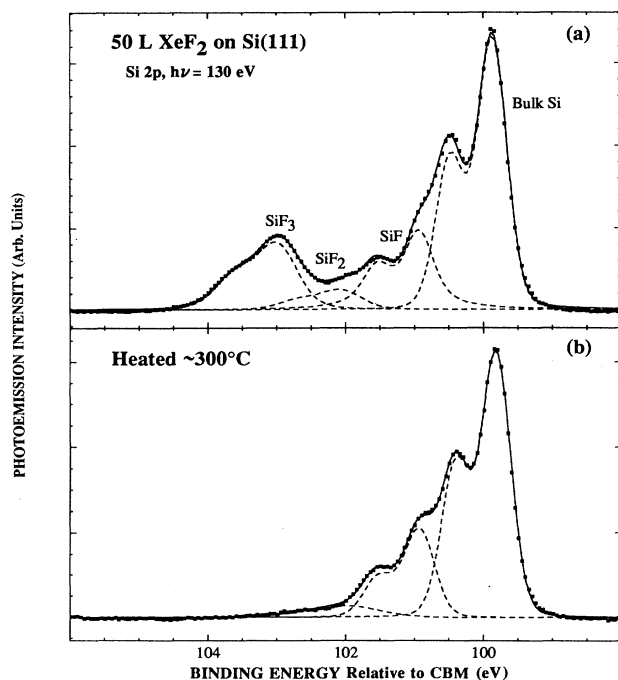


FIG. 1. Photoemission spectra of the Si 2*p* core level of a Si(111) surface after exposure to 50 L of XeF<sub>2</sub> at (a) room temperature and (b) after annealing to  $\sim 300^\circ\text{C}$ , collected with 130 eV photon energy. The raw data, after subtraction of a background, are shown by the squares. The solid lines are the result of a numerical fit to the data, and the dashed lines are the individual components of the fit (see text).

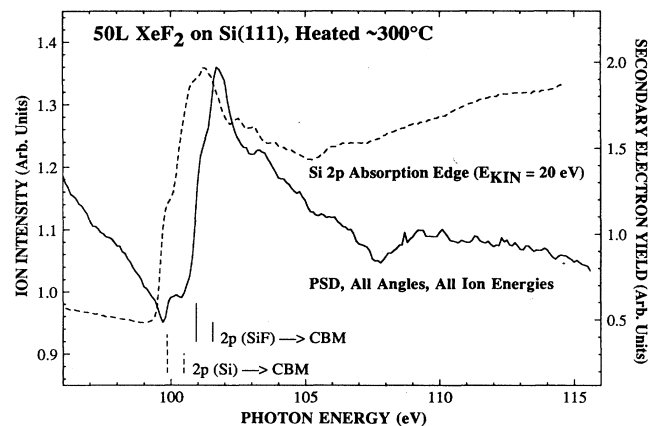


FIG. 2. Absorption and PSD yield at the Si 2*p* edge for a Si(111) surface after exposure to 50 L of XeF<sub>2</sub> at room temperature followed by annealing to  $\sim 300^\circ\text{C}$  [same surface as in the photoemission spectrum in Fig. 1(b)]. The absorption (dashed line) was collected by monitoring the yield of 20-eV secondary electrons as a function of the photon energy. The PSD (solid line) was collected over all emission angles (bias voltage on) by monitoring ions desorbed at all kinetic energies. The intensity scale refers to the PSD data. The vertical lines correspond to the transitions from the bulk Si 2*p* level (dashed lines) and from the 2*p* level in a SiF unit (solid lines) to the CBM. The splitting of the vertical lines represents the spin-orbit splitting of the 2*p* core level.

energy was chosen in order to maximize the surface sensitivity of the measurement, since 20 eV is approximately the energy at which the inelastic mean free path for electrons traveling through silicon is minimized (about 5 Å).<sup>14</sup> However, the secondary-electron signal contains a large contribution of electrons that are the result of a cascade of inelastic processes originating from a depth many times that of the inelastic mean free path. The absorption spectrum in Fig. 2 is therefore more bulk sensitive than one would desire for studies of monolayer quantities of adsorbates, but it is as surface sensitive a measurement as is possible when employing secondary electrons to monitor absorption.

The edge at  $\sim 100$  eV in the absorption spectrum results from electrons excited from the  $2p$  core level of bulk silicon to the conduction-band minimum (CBM).<sup>14,15</sup> The structure seen on the edge results from the spin-orbit splitting of the  $2p$  level. The thresholds for this process are illustrated by the dashed vertical lines in Fig. 2, which were obtained from the photoemission data. The absorption from the  $2p$  level in the first-layer Si atoms bonded to fluorine (which are shifted  $\sim 1$  eV higher in binding energy than the bulk Si) also contributes to the measured absorption spectrum, and the positions of the thresholds for these transitions are illustrated in Fig. 2 by the solid vertical lines. However, since we are sampling all of the Si atoms visible with this detection technique, the absorption of the first-layer atoms is obscured by the bulk absorption signal.

The PSD spectrum of the annealed surface, collected by monitoring all of the desorbing ions, is shown in Fig. 2 as a solid line. This spectrum shows a small structure at approximately the same photon energy as the absorption edge ( $\sim 100$  eV), and shows a much larger edge shifted towards higher photon energies by  $\sim 1$  eV. The small edge seen at  $\sim 100$  eV in the PSD curve is the result of ESD induced by the secondary electrons created by absorption of photons at the bulk Si  $2p$  edge.<sup>16</sup> Electrons which cause ion desorption via this indirect process do so through excitation of lower-lying core-level or valence states. Since the number of secondary electrons created is proportional to the absorption, this indirect process should produce a curve essentially identical to the total absorption spectrum of the surface. Note that the indirect PSD edge in the raw data appears to peak at a lower photon energy than the corresponding absorption spectrum. This is due largely to distortions in the peak shape which result from the considerably steeper background associated with the PSD spectrum.

The large edge at  $\sim 101$  eV (which peaks at  $\sim 102$  eV) results from the direct excitation of an electron from the  $2p$  level of the bonding Si atom in a monofluoride unit to the CBM.<sup>4</sup> The position and structure of this edge correlate well with the solid vertical lines that illustrate the onset of the transition. As is evident by comparison of the intensities of the direct and indirect PSD edges, the direct excitation of the bonding Si atom is a more likely process than the indirect excitation (by about an order of magnitude) for inducing PSD at the Si  $2p$  core level.

Note that the entire  $2p$  PSD edge is riding on a background of desorbed-ion signal (the intensity at the 102-eV

peak is about 50% higher than the intensity just before the edge). This background results from both the direct excitation of lower-lying core levels and ESD induced by electrons photoemitted from the sample, in a similar manner to the indirect peak discussed above. For the silicon-on-fluorine system, the threshold for stimulated desorption correlates with the F  $2s$  level at 27.5 eV, indicating that valence excitations do not give rise to ESD of  $F^+$ .<sup>9</sup> As there are no core levels located between the F  $2s$  and the Si  $2p$ , the background signal prior to and underneath the  $2p$  edge must arise primarily from excitation (directly by the photons and indirectly by secondary electrons) of the F  $2s$  level. There is also some contribution to the background ion signal from second- and higher-order light, however, which is sufficiently energetic to directly excite the Si  $2p$  level.

The direct processes proceed via a mechanism that begins with the removal of a Si  $2p$  core electron by the absorption of a photon. The resulting excited electronic state decays by an interatomic Auger process, leading to the formation of a two-hole state on the F atom. Because the bonding of the F atom is fairly ionic, i.e., fluorine is initially in a  $F^-$  oxidation state, two holes are needed to produce a  $F^+$  ion. This two-hole state is the localized excited final state whose repulsive potential is responsible for the emission of an ion. This final state must have a sufficiently long lifetime to allow the fluorine ion to escape the surface. Note that the details of this repulsive potential determine the kinetic energy of the desorbing ion.

The peak at  $\sim 102$  eV in the PSD spectrum of Fig. 2 is a single, narrow feature whose width is comparable to the SiF component of the photoemission spectrum. The position of this peak indicates that the ions observed in this spectrum are emitted in a direct process via excitation of the Si  $2p$  level at a monofluoride surface site. The narrow width of the peak indicates the absence of any significant structure in the localized density of unoccupied states associated with a monofluoride moiety. Since the probability for PSD in this process is proportional to the absorption of a photon by the Si  $2p$  core level, the PSD spectrum provides an absorption spectrum localized at the bonding atom. Our previous comparison of the difference between a clean-surface absorption spectrum and a spectrum obtained from a monofluoride-covered surface had shown that the PSD in this case was a good measure of single-atom absorption.<sup>4</sup>

The second surface employed for these studies was prepared by a 50-L dose of  $XeF_2$  without annealing. In addition to silicon monofluoride, this surface has a significant number of trifluoride species on the surface, as shown in Fig. 1(b). The PSD spectrum collected at the Si  $2p$  edge from this surface is shown by the solid line in Fig. 3, while the PSD spectrum of the annealed surface is shown as a dashed line for comparison. The difference between the spectra collected from the unannealed and annealed surfaces is representative of the PSD excitation spectrum for  $F^+$  ions originating at a  $SiF_3$  site. The PSD excitation curve for  $F^+$  originating from a  $SiF_3$  group is not simply a single peak shifted to higher photon energy; in addition to the edge at  $\sim 103$  eV, which correlates with

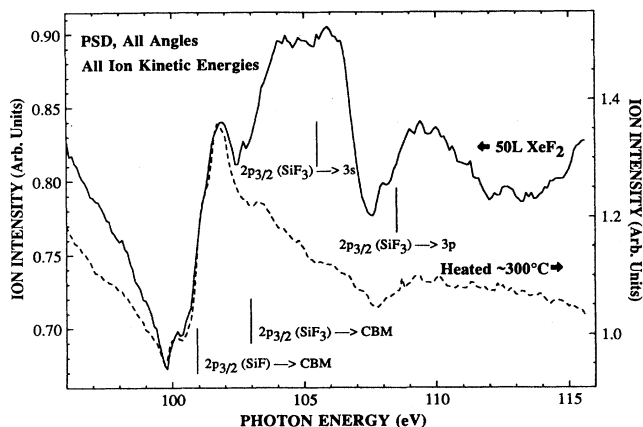


FIG. 3. PSD collected over all emission angles (bias voltage on) by monitoring ions desorbed at all kinetic energies for a Si(111) surface exposed to 50 L of  $\text{XeF}_2$  (solid line) and followed by annealing to  $\sim 300^\circ\text{C}$  (dashed line). The spectrum represented by the dashed line in this figure is the same as the solid line in Fig. 2. The solid vertical lines correspond to the transitions from the Si  $2p_{3/2}$  level in a SiF or  $\text{SiF}_3$  unit to either the CBM or a 3s- or 3p-like final state. The transitions from each of the corresponding  $2p_{1/2}$  core levels are not shown in order to reduce the clutter in the figure.

the direct excitation of an electron from the  $2p$  level in a  $\text{SiF}_3$  group to the CBM, the PSD spectrum from  $\text{SiF}_3$  shows structure at higher incident-photon energies.

The additional structure in the PSD spectrum observed prior to annealing results from excitations of electrons from the  $2p$  level of a  $\text{SiF}_3$  surface species to localized molecular-orbital-like ( $\sigma^*$ ) states that are formed via "inner-well" resonances<sup>17</sup> in the quasimolecular  $\text{SiF}_3$ .<sup>4</sup> These states have sufficient atomic character that they can be labeled as Rydberg-like Si 3s and 3p states. The assignment of these features is based on the correspondence (within 0.2 eV) between these data and the positions of the corresponding transitions seen in gas-phase and condensed  $\text{SiF}_4$ .<sup>18,19</sup> Solid vertical lines are shown in Fig. 3 that represent the thresholds for these transitions. (The positions of the lines of the 3s and 3p states were chosen directly from the data of Fig. 3, and are not an independent measure of the positions of these states.) The difference between the unannealed and annealed surfaces provides a localized absorption spectrum of a  $\text{SiF}_3$  surface site. Care should be exercised, however, in interpreting the shape of this curve as being identical to the  $\text{SiF}_3$  absorption coefficient. As will be discussed below, the details of the particular electronic states involved in the initial excitation can severely effect the probability for PSD.

In Fig. 4 the spectra collected for the unannealed surface are shown both with (solid line) and without (dashed line) the bias voltage. The bias voltage was chosen to be large enough to collect the ions emitted in all directions. By turning the bias voltage off, the signal due to ions emitted from the sample along grazing exit directions is attenuated, roughly those ions emitted at angles greater

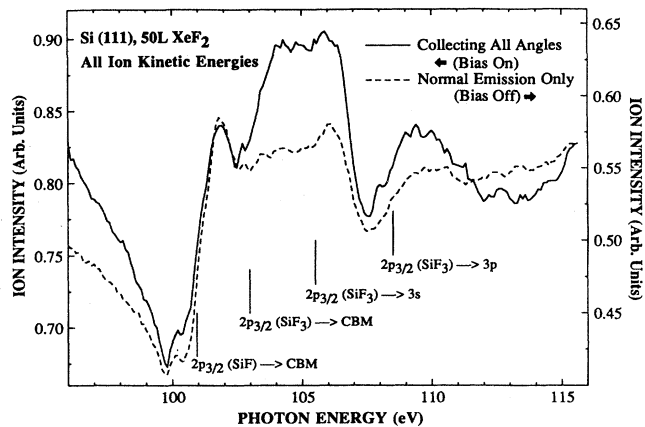


FIG. 4. PSD collected by monitoring ions desorbed at all kinetic energies for a Si(111) surface exposed to 50 L of  $\text{XeF}_2$ . The solid line represents ions collected over all emission angles (bias on), and the dashed line represents those ions desorbed primarily in the normal direction (bias off). The spectrum represented by the solid line in this figure is the same as the solid line in Fig. 3.

than  $45^\circ$  from the surface normal. In Fig. 4 the raw data are displayed with a constant added to the bias-off spectrum to account for the loss of background ions which were desorbed in off-normal directions via secondary processes. This allows the intensities underneath the bias-on and bias-off  $2p$  edges to be directly compared to each other. The data in Fig. 4 show that the intensity of the edge due to direct desorption from SiF surface sites is independent of the bias voltage, indicating that all of the  $\text{F}^+$  originating from SiF surface species is desorbed within  $45^\circ$  of the surface normal. Conversely, since only the emission of  $\text{F}^+$  from  $\text{SiF}_3$  groups is enhanced with the application of the bias voltage, these ions are the only ions which desorb at angles greater than  $45^\circ$  from the surface normal.

It has been well established that ions desorbing via an ESD (Ref. 20) or PSD (Ref. 12) process exit the sample along a direction related to the initial bond angle on the surface. Our results therefore indicate that the bond direction in a SiF species is directed towards the surface normal, while the bond direction in a  $\text{SiF}_3$  species is not. This is a reasonable expectation for Si(111)-(7 $\times$ 7) surfaces covered with approximately monolayer amounts of fluorine. The first species to adsorb on the surface would tie up the dangling Si bonds, which are pointed normal to the surface, and form monofluorides. Further exposures would then serve to break Si—Si bonds in order to form higher fluorides. The Si atom of a trifluoride group would be bonded to the surface via a Si—Si bond, which would be normal to the surface because of the (111) crystal symmetry. The Si—F bonds, which form the remaining three corners of a tetrahedron, would then be approximately  $70^\circ$  from the surface normal.

Studies of the etching rate of Si with  $\text{XeF}_2$  have indicated that, at a 50-L exposure, etching of the substrate has already begun.<sup>21</sup> The major reaction product from

the etching of Si with  $\text{XeF}_2$  is  $\text{SiF}_4$ , and the  $\text{SiF}_2$  and  $\text{SiF}_3$  seen on the surface are reaction intermediates formed during the etching process.<sup>13,22</sup> In contrast to the data of Refs. 13 and 22, however, at this exposure level the surface has not reached equilibrium steady-state etching, and the thick reaction layer characteristic of steady-state etching has not yet formed. The data of Ref. 21 indicate that after a 50-L exposure approximately 20 monolayers of silicon would already have been stripped away. Since our angularly resolved results show that there is substantial order to the silicon fluoride species present after a 50-L dose, at this exposure level etching must proceed in a quasi-layer-by-layer fashion.

Note that the bias-off spectrum shown as the dashed line in Fig. 4 differs from the spectrum shown in Fig. 3 of Ref. 4 in that no emission from  $\text{SiF}_3$  groups was seen in the earlier work, despite the fact that the same surface preparation was used in both cases. The difference in the "Normal PSD" curve in Fig. 3 of Ref. 4 and the dashed line in Fig. 4 of the present paper lies in the difference in the ion kinetic energies over which the data were collected. In Ref. 4 ions were collected with kinetic energies of  $2.20 \pm 1.25$  eV, while in the present case data were collected for kinetic energies of  $4.00 \pm 4.50$  eV. Although this may appear to be a trivial point, since the majority of the desorbed ions are collected in both cases, the PSD spectra are actually quite sensitive to the kinetic energies over which the ions are collected. The following discussion addresses this point.

Kinetic-energy distributions of the desorbed ions are shown in Fig. 5. Since there is no *a priori* understanding of the relative contributions of the individual PSD processes to the overall kinetic-energy distributions, they have been simply normalized to equal peak heights for the figure. The overall shapes of these kinetic-energy distributions are qualitatively similar, showing maxima at  $\sim 2.2$  eV, in agreement with the measurements of Bozack *et al.*<sup>9</sup> Figure 5(a) shows a comparison of the data from the annealed and unannealed surfaces at a photon energy of 109.2 eV, and also compares the data collected from the unannealed surface with the bias voltage on and off. This photon energy was chosen because it accentuates desorption from  $\text{SiF}_3$  species. Turning off the bias voltage with an unannealed surface has the effect of reducing the contribution of desorbed ions from  $\text{SiF}_3$  surface sites relative to  $\text{SiF}$  sites. A further reduction in the contribution of  $\text{F}^+$  from  $\text{SiF}_3$  species is obtained by annealing the surface. These data show that as the contribution of fluorine ions from  $\text{SiF}$  species is increased relative to the contribution from  $\text{SiF}_3$  species, the kinetic-energy distribution becomes narrower. Thus, the kinetic-energy distribution of ions originating from  $\text{SiF}_3$  species is broader than the distribution of ions originating from  $\text{SiF}$  sites.

In Fig. 5(b) kinetic-energy distributions from the unannealed surface using three different incident-photon energies are displayed. These photon energies correspond to the transitions from the Si  $2p$  level in a  $\text{SiF}$  group to the CBM (101.7 eV), from the Si  $2p$  level in a  $\text{SiF}_3$  group to the CBM (103.7 eV), and from the Si  $2p$  level in a  $\text{SiF}_3$  group to the  $3p$ -like state (109.2 eV). Note that the ma-

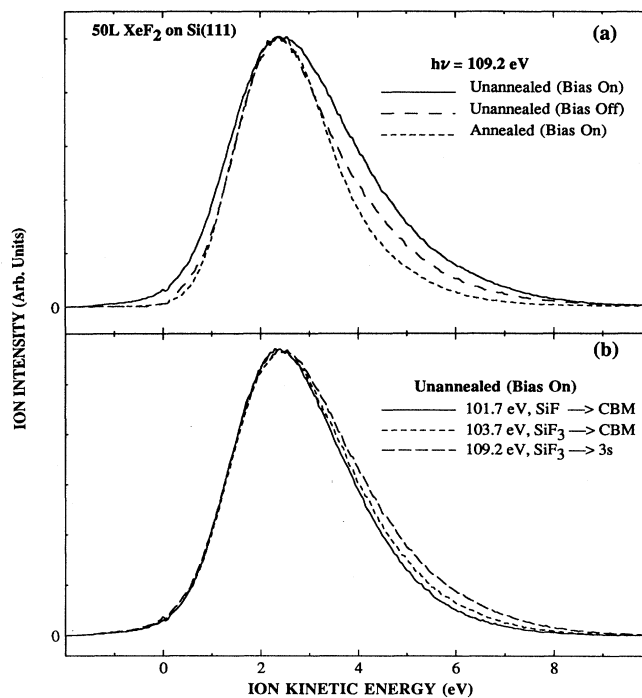


FIG. 5. Kinetic-energy distributions of fluorine ions desorbed from a Si(111) surface exposed to 50 L of  $\text{XeF}_2$ , and from that surface after annealing to 300 °C.

majority of the ions measured in these kinetic-energy distributions have been desorbed via secondary (background) processes, which accounts for the almost quantitative similarity of the distributions. There are higher-kinetic-energy components, however, seen with initial excitations of the  $\text{SiF}_3$  species that are not present when desorbing from the  $\text{SiF}$  initial state. Since the contribution from the background processes is unaffected by the incident-photon energy, the small differences in the distributions represent much larger actual differences between the distributions associated with each of the direct photodesorption processes.

The differences in the ion kinetic-energy distributions are a result of the combined effects of a number of independent factors. The initial kinetic energy is determined by the shape of the repulsive potential of the final state of the ion as it desorbs from the surface, and the details of this potential are a function of the local bonding of the adsorbate and of the electronic structure of the particular excitation. Secondly, the kinetic energy of an ion may be modified as it escapes the surface. Because of the complicated and interdependent nature of the various contributions to the kinetic-energy distributions, our observations cannot be attributed to a single effect. We can, however, identify some of the important effects, and suggest how these manifest themselves in the data.

A possible contribution to the broadening of the ion kinetic-energy distributions originating from  $\text{SiF}_3$  surface species arises from the extra vibrational modes available to a  $\text{SiF}_3$  moiety as compared to  $\text{SiF}$ . The measured full

width at half maximum for ions originating from  $\text{SiF}_3$  is broadened by approximately an additional 1.5 eV over ions originating from  $\text{SiF}$  [Fig. 5(a)]. Although, at room temperature, only the ground-state vibrational levels are appreciably populated, these modes could be excited via processes occurring as a result of the absorption of photons and the subsequent creation of a cascade of secondary electrons. For example, low-energy secondary electrons may be absorbed at a  $\text{SiF}_3$  site, inducing a transition to a higher vibrational level. If higher vibrational modes were populated in a bound species, then the excitations which result in PSD could occur from these levels to a wider region of the repulsive potential than would be available from the ground state. This would have the effect of broadening a measured ion kinetic-energy distribution. Note that such a broadening of ion kinetic-energy distributions due to (thermal) population of excited vibrational energy levels has been previously observed for ESD of  $\text{O}^+$  desorbing from tungsten.<sup>23</sup>

The results shown in Fig. 5 indicate that not only are the ion kinetic-energy distributions broader for ions originating from  $\text{SiF}_3$ , but they are also shifted towards higher energy. This is directly evident in the data presented in Fig. 5(b) (compare the 101.7-eV excitation to the 103.7-eV excitation), since the contribution from background processes is the same at these two photon energies. There are two factors which may contribute to a higher kinetic-energy distribution for ions originating from a  $\text{SiF}_3$  site over a  $\text{SiF}$  site apart from broadening due to vibrations.

As mentioned above, the ions originating from a  $\text{SiF}_3$  species are desorbed along more grazing exit directions than ions originating from the monofluoride surface species. As has been seen by Stulen,<sup>24</sup> and predicted by calculation,<sup>25</sup> ions desorbing at grazing angles require more kinetic energy to overcome the attraction of the ion by its image potential than ions exiting in the normal direction from a surface. This will result in the removal from the ion yield of the ions with the lowest kinetic energies. In addition, the probability for reneutralization of ions should also increase at grazing angles. Since our detector is only sensitive to that fraction of desorbed species which remains charged, the removal of low-kinetic-energy ions from the ion yield via either attraction by the image potential or by electron transfer from the solid will result in an apparent shift of the measured ion kinetic-energy distribution towards higher values.

A second factor which can contribute to a higher-kinetic-energy distribution for ions originating from  $\text{SiF}_3$  surface species is the increased Coulomb repulsion that a  $\text{F}^+$  ion would feel with respect to silicon in a 3+ oxidation state over a 1+ oxidation state. Williams and Gillen<sup>26</sup> have seen Coulombic effects in comparisons of  $\text{F}^+$  and  $\text{F}^{2+}$  ESD from aluminum. In our case, however, it is the cation and not the anion that is in a higher oxidation state. If Coulomb repulsion were dominant, then a three-fold increase in kinetic energy would be expected from a  $\text{Si}^{3+}$  initial state over a  $\text{Si}^{1+}$  initial state. However, the actual ionicity of a  $\text{Si}-\text{F}$  bond is incomplete,<sup>27</sup> and the Coulomb force felt between a  $\text{F}^+$  ion and a silicon cation would be screened by the bonding electrons and reduced

by the presence of the other (negatively charged) fluorine atoms in the  $\text{SiF}_3$  group. These effects would act to decrease the Coulomb repulsion felt by the desorbing ion, and therefore any increase in the ion kinetic energies induced by Coulombic repulsion is likely to be small.

In Fig. 5(b) it is also seen that there is a higher-kinetic-energy component in the distribution obtained with the excitation from the  $2p$  initial state in a  $\text{SiF}_3$  unit to the  $3p$ -like empty state (109.2 eV) that is not present when using an excitation to just above the CBM (103.7 eV). [The kinetic-energy distribution for excitation to the  $3s$  empty state (not shown) is indistinguishable from the transition to the  $3p$  state.] This phenomenon cannot be understood via either of the arguments postulated above to explain the kinetic-energy increase for an ion originating from a  $\text{SiF}_3$  surface site over a  $\text{SiF}$  site, since these ions have all originated from the same surface species and were therefore in the same initial electronic configuration. This result indicates that the potential of the repulsive final state obtained after excitation to a molecular-orbital-like electronic state is different (steeper) than that obtained after removing a  $2p$  electron via a transition to the CBM. That the repulsive potential of the final state is dependent on the initial excitation can be rationalized in the following manner. With an excitation to the CBM, the initially excited electron is delocalized in the conduction band forming a two-hole (2h) final state. In contrast, an excitation to a molecular-orbital-like state leads to a two-hole one-electron (2h-1e) final state in which the excited electron remains localized in the  $3p$ -like (or  $3s$ -like) orbital long enough to affect the potential responsible for the desorption of  $\text{F}^+$ . The importance of various types of final states has been discussed in detail by Ramaker.<sup>28</sup>

In Fig. 5 it is evident that the unoccupied electronic state involved in the initial excitation affects the kinetic energy of an ion. This effect does not dominate the data, however, since about two-thirds of the events in each of the kinetic-energy distributions are the result of the secondary processes which comprise the background underneath the  $2p$  edge. The delineation of the various contributions to the ion kinetic energy is more readily observed via measurements of the PSD yield versus photon energy obtained by monitoring only those ions which have desorbed at a particular kinetic energy. Figure 6 shows the spectrum obtained by monitoring all ions (which is the same spectrum as the solid lines in Figs. 3 and 4), as well as the spectrum obtained by monitoring ions with very high ( $7.5 \pm 2.5$  eV) kinetic energies. These data have been normalized at the edge due to direct excitation of  $\text{SiF}$  (at  $\sim 102$  eV) in order to easily observe the changes in the ratio of the PSD originating from a  $\text{SiF}_3$  group to the PSD from a  $\text{SiF}$  group.

It is clear from the data in Fig. 6, which show the PSD spectrum obtained for ions with high kinetic energies, that the particular electronic state associated with the initial excitation has a strong effect on the kinetic energy of the desorbed ions. Not only is the intensity of the features associated with removal of  $\text{F}$  from  $\text{SiF}_3$  species increased with respect to the  $\text{SiF}$ -derived features, but the intensity of the features resulting from excitation from the  $\text{SiF}_3$   $2p$  initial state to the molecular-orbital-like states

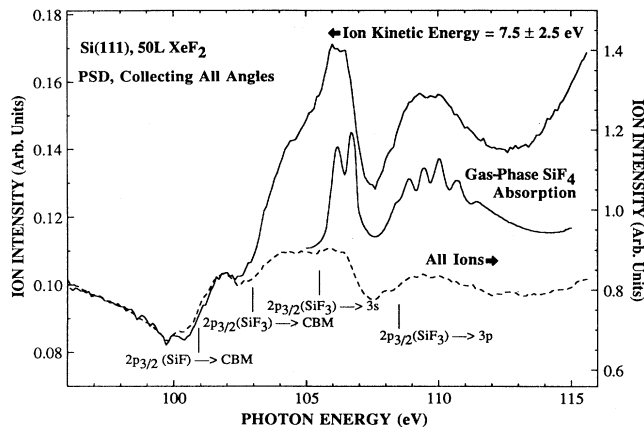


FIG. 6. PSD collected over all emission angles (bias voltage on) from a Si(111) surface exposed to 50 L of XeF<sub>2</sub> and gas-phase absorption of SiF<sub>4</sub> from Ref. 19. The PSD spectra represent ions collected over all kinetic energies (long dashes) and at  $7.5 \pm 2.5$  eV (solid line). The spectrum represented by the long dashes in this figure is the same as the solid lines in Figs. 3 and 4.

are increased relative to the feature resulting from the excitation from the SiF<sub>3</sub> 2*p* initial state to the CBM, consistent with the results of Fig. 5.

Also shown in Fig. 6 is the gas-phase absorption spectrum of SiF<sub>4</sub> from Ref. 19. The agreement in the energetic positions of these transitions is within the accuracy of the monochromator to obtain an absolute measurement. That there is little change in the relative positions of the 2*p*, 3*s*, and 3*p* levels in going from adsorbed SiF<sub>3</sub> to gaseous SiF<sub>4</sub> indicates the largely atomic character of these energy levels. The structure seen in the gas-phase spectrum is a result of the spin-orbit splitting of both the 2*p* and 3*p* states. This structure is visible in the PSD spectra, but the transitions in the PSD spectra are broadened by the interaction of the SiF<sub>3</sub> adsorbate species with the substrate. This broadening is likely due to coupling of the molecular vibrations to the transition, which is also observed with SiF<sub>4</sub>.<sup>19</sup>

The enhancement of the transitions to the molecular-orbital states, which occurs when monitoring ions at high kinetic energies, can be exploited as a means for verifying the specific atomic-like character of these states. This is demonstrated in Fig. 7, where the PSD spectra for the 2*p* edge are compared with the PSD obtained at the 2*s* edge. Normally, the intensity at the 2*s* edge is weak and there is a significant background due to direct excitation of the 2*p* level and to ESD induced by electrons created by absorption at the 2*p* level. By monitoring those ions with  $7.5 \pm 2.5$  eV kinetic energy, however, the transitions to the 3*s* and 3*p* final states are enhanced sufficiently so that they become visible above the background. Optical selection rules predict that pure 2*p* → 3*p* and 2*s* → 3*s* transitions are forbidden (i.e.,  $\Delta l \neq 0$ ). These levels are not pure atomic states, however, but are merely labeled by the predominant atomic character of the molecular orbital. What is observed in the data of Fig. 7 is that the ratio

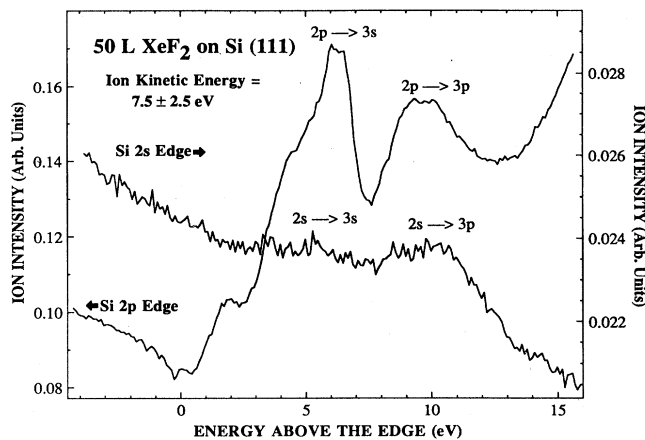


FIG. 7. PSD collected over all emission angles (bias voltage on) at the Si 2*s* and Si 2*p* edges for ions desorbing with  $7.5 \pm 2.5$  eV kinetic energy from a Si(111) surface exposed to 50 L of XeF<sub>2</sub>. The transition from the bulk Si 2*s* or 2*p*<sub>3/2</sub> initial state to the conduction band was taken as the zero of energy.

of intensities of the 3*s* and 3*p* final states reverse in going from the 2*p* to the 2*s* initial state. This is consistent with the assignment of predominantly 3*s* and 3*p* character to these molecular-orbital-like states.

#### IV. CONCLUSIONS

The desorption of F<sup>+</sup> from Si(111) has been studied employing photon energies in the region of the Si 2*p* and 2*s* edges. These studies have shown that the PSD at the 2*p* edge is dominated by direct excitations of the bonding Si atoms, and is therefore dependent on the oxidation state of the bonding atom. This has been used to perform localized absorption spectroscopy of individual SiF and SiF<sub>3</sub> moieties. While the absorption associated with SiF species shows little structure, 3*s* and 3*p* Rydberg-like resonances have been observed localized at the quasimolecular SiF<sub>3</sub> surface sites. Desorption from SiF sites occurred exclusively along the surface normal, while ions originating from SiF<sub>3</sub> sites desorbed primarily along grazing angles.

Measurements of the kinetic-energy distributions of the desorbing fluorine ions have been used to delineate the mechanisms leading to PSD, which are dependent on the details of both the occupied and unoccupied electronic states involved in the initial excitation. Kinetic-energy distributions of ions desorbed from SiF<sub>3</sub> sites are broader and shifted to slightly higher kinetic energy than ions desorbed from SiF sites. In addition, ions desorbed via an initial excitation to either the 3*s*- or 3*p*-like state have an even higher kinetic energy. PSD spectra collected by monitoring only high-kinetic-energy ions were used to enhance the relative intensity of the 2*p* and 2*s* edges associated with SiF<sub>3</sub>. Since the absolute PSD yield may also be affected by the details of the initial electronic transition, care must be exercised in concluding that a PSD spectrum represents a quantitative measure of single-atom absorption.

## ACKNOWLEDGMENTS

This research was carried out at the National Synchrotron Light Source (NSLS), Brookhaven National Laboratory (Upton, NY), which is supported by the Division of Materials Sciences of the Office of Basic Energy Sciences, U.S. Department of Energy. The authors

wish to acknowledge Professor T. E. Madey and Dr. L. J. Whitman for useful discussions, and Dr. F. R. McFeely and the staff of IBM beamline UV-8 at NSLS for their assistance. One of us (S.A.J.) acknowledges the National Academy of Science and National Research Council (NAS/NRC) for partial support.

- 
- \*Formerly the U.S. National Bureau of Standards.
- <sup>1</sup>T. E. Madey, D. E. Ramaker, and R. Stockbauer, *Annu. Rev. Phys. Chem.* **35**, 215 (1984).
- <sup>2</sup>M. L. Knotek, *Rep. Prog. Phys.* **47**, 1499 (1984).
- <sup>3</sup>D. Menzel, *Nucl. Instrum. Methods Phys. Res., Sect. B* **13**, 507 (1986).
- <sup>4</sup>J. A. Yarmoff, A. Taleb-Ibrahimi, F. R. McFeely, and Ph. Avouris, *Phys. Rev. Lett.* **60**, 960 (1988).
- <sup>5</sup>F. R. McFeely, J. F. Morar, N. D. Shinn, G. Landgren, and F. J. Himpsel, *Phys. Rev. B* **30**, 764 (1984).
- <sup>6</sup>F. J. Himpsel, D. E. Eastman, P. Heimann, B. Reihl, C. W. White, and D. M. Zehner, *Phys. Rev. B* **24**, 1120 (1981).
- <sup>7</sup>D. E. Eastman, J. J. Donelon, N. C. Hein, and F. J. Himpsel, *Nucl. Instrum. Methods* **172**, 327 (1980).
- <sup>8</sup>Ph. Avouris, F. Bozso, and A. R. Rossi, in *Photon, Beam and Plasma Stimulated Chemical Processes at Surfaces*, edited by V. M. Donnelly, I. P. Herman, and M. Hirose (Materials Research Society, Pittsburgh, PA, 1987), p. 591.
- <sup>9</sup>M. J. Bozack, M. J. Dresser, W. J. Choyke, P. A. Taylor, and J. T. Yates, Jr., *Surf. Sci.* **184**, L332 (1987).
- <sup>10</sup>J. A. Yarmoff and S. A. Joyce (unpublished).
- <sup>11</sup>T. E. Madey and R. Stockbauer, *Methods Expt. Phys.* **22**, 465 (1985).
- <sup>12</sup>T. E. Madey, R. Stockbauer, J. F. van der Veen, and D. E. Eastman, *Phys. Rev. Lett.* **54**, 187 (1980).
- <sup>13</sup>F. R. McFeely, J. F. Morar, and F. J. Himpsel, *Surf. Sci.* **165**, 277 (1986).
- <sup>14</sup>F. J. Himpsel, P. Heimann, T.-C. Chiang, and D. E. Eastman, *Phys. Rev. Lett.* **45**, 1112 (1980).
- <sup>15</sup>W. Eberhardt, G. Kalkoffen, C. Kunz, D. Aspnes, and M. Cardona, *Phys. Status Solidi B* **88**, 135 (1978).
- <sup>16</sup>D. E. Ramaker, T. E. Madey, R. L. Kurtz, and H. Sambe, *Phys. Rev. B* **38**, 2099 (1988).
- <sup>17</sup>A. Bianconi, *Surf. Sci.* **89**, 41 (1979).
- <sup>18</sup>R. A. Rosenberg, *J. Vac. Sci. Technol. A* **2**, 1463 (1986).
- <sup>19</sup>H. Friedrich, B. Pittel, P. Rabe, W. H. E. Schwarz, and B. Sonntag, *J. Phys. B* **13**, 25 (1980).
- <sup>20</sup>T. E. Madey, *Science* **234**, 316 (1986).
- <sup>21</sup>H. F. Winters and D. Haarer, *Phys. Rev. B* **36**, 6613 (1987).
- <sup>22</sup>J. A. Yarmoff and F. R. McFeely, *Phys. Rev. B* **38**, 2057 (1988).
- <sup>23</sup>T. E. Madey and J. T. Yates, Jr., *J. Chem. Phys.* **51**, 1264 (1969).
- <sup>24</sup>R. H. Stulen, in *Desorption Induced by Electronic Transitions DIET II*, edited by W. Brenig and D. Menzel (Springer-Verlag, Berlin, 1985), p. 130.
- <sup>25</sup>Z. Miskovic, J. Vulkanic, and T. E. Madey, *Surf. Sci.* **141**, 285 (1984).
- <sup>26</sup>P. Williams and G. Gillen, *Surf. Sci.* **180**, L109 (1987).
- <sup>27</sup>M. Seel and P. S. Bagus, *Phys. Rev. B* **28**, 2023 (1983).
- <sup>28</sup>D. E. Ramaker, in *Desorption Induced by Electronic Transitions DIET II*, edited by W. Brenig and D. Menzel (Springer-Verlag, Berlin, 1985), p. 10.